OPTICAL CHARACTERIZATION OF ULTRATHIN SILICON SUBSTRATES

T. GLOBUS*, S. H. JONES*, and T. DIGGES, Jr.**
* EE Department, University of Virginia, Charlottesville, VA 22903
**Virginia Semiconductor Inc, Fredericksburg, VA 22401

ABSTRACT

In this paper we present results for the absorption coefficient and refractive index spectra of p- and n-type silicon membranes doped with phosphorous or boron at different levels. These results cover the wide energy range from 0.5 eV up to 2.5 eV, thus including effects of subgap defect and impurity absorption, and the range of possible transitions to higher conduction band minima. The results have been obtained by utilizing both a conventional transmission and reflection measurement technique at small values of transmittance, and a recently developed optical interference spectroscopy characterization technique. The results in the visible and near infrared regions from the two techniques have been compared, and the range of transmission where the conventional technique is applicable have been determined. The preliminary analysis of these data indicate that a new information regarding the Si electronic band structure can be extracted.

INTRODUCTION

Ultrathin single crystal silicon membranes respond to the needs of the rapidly developing micromachining industry, the research needs within the traditional microelectronics industry, and photonic, X-ray, and optics applications. These applications require dimensional stability in flatness and surface planarity. Material preparation is based on growing of Czochralski single crystal silicon with the range of dopants which covers the normal spectrum of Boron, Phosphorus, Arsenic and Antimony, as well as undoped silicon. Ultrathin silicon membranes are made to thicknesses as low as 4 microns. They are double side polished, and are extremely flexible due to the dominance of the elastic nature of single crystal silicon. The thickness tolerance range for all membranes, up to 20 microns, remains at +/- 1 micron. Ultrathin and Ultramachining silicon wafers are well suited for microcircuit devices, however, their functional uses extend far beyond this limited field as being a substrate, and include mechanical and chemical sensors, silicon on insulator (SOI) devices (ultra- Machining wafers are available with or without SiO_2), infrared and interference filters, visible light detectors and micromachined detector arrays, controlled breakdown voltage diodes and voltage multipliers, X-ray reflectors and focusing mirrors. Additional benefits are derived from having both sides polished, therefore circuits can be patterned on both side of a wafer. Thicknesses of 20-22 microns are arrived at by a chemical/ mechanical polishing process. Chemical polishing procedures achieve double side polished thinnesses in the 4 μm range. These wafers have low damage due to the slow removal rate of Si processing (about 50 μm per hour). To address concerns related to micro-roughness, an additional production step often follows standard polishing. This "hase-free" step produces the surface smoothness of membranes in the 3-7 angstrom range. Typically ultra thin wafers have 8-20 Å of micro-roughness.

For many applications, the superior precision in controlling wafer planarity, surface texture, thickness uniformity is sufficient and enough. However, in other microelectronic and photonic applications there are new requirements outside of the more traditional silicon fields. The knowledge of absorption coefficient and refractive index spectra are extremely important for all optoelectronic devices. Optical properties of ultrathin silicon membranes have to be studied to provide necessary information.

Although silicon is the main material in microelectronics, and it was studied for many, many years, there are still open questions. One of such questions is related to position of higher conduction band minima. The second conduction band minima (approximately at X points of the Brillouin zone along the X - K direction) and the higher minima along the [111] axes known from calculations of Si band structure are relatively close in energy to the absolute minima along the Γ-X axes (0.2-1 eV) *[1]*. However, these features have not been accurately determined in experiments and until now there is no agreement regarding the second and the third indirect band

Mat. Res. Soc. Symp. Proc. Vol. 485 © 1998 Materials Research Society

gap. This information can be important for engineering and for accurately modeling high energy effects in new type microelectronic and photonic silicon devices.

There were a number of recent reports on the absorption coefficient of silicon *[2, 3].* However, excellent wafer planarity and thickness uniformity make it difficult to use conventional transmission measurements for optical characterization of thin Si wafers because of interference effects. Reflection from the back surface induce significant errors in refractive index and absorption coefficient values obtained by using conventional technique, even in the range of relatively small optical transmission, where interference is not visible. In this paper we present results of optical characterization of ultrathin silicon wafers by utilizing both, conventional transmission and reflection measurements technique at small values of transmittance, and recently developed optical interference spectroscopy characterization technique *[4, 5].* This new technique is based on a self-consistent data-analysis algorithm for simultaneously measured optical transmission and specular reflection, using exact interference equations. Precise spectra of absorption coefficient and refractive index of N- and P- type samples doped with different concentrations of Phosphorus and Boron have been measured in a wide energy range, thus including effects of intrinsic subgap defect and impurity absorption and the range of possible transitions to higher conduction band minima. We compared results from two techniques in the visible and near infrared regions and have determined the range of transmission where conventional technique is applicable. The analysis of the data indicate that chemical polishing possibly effects subgap absorption.

EXPERIMENTAL TECHNIQUE

In this study, we used conventional transmission and reflection measurements technique at small values of transmittance, and interference spectroscopy technique which was recently demonstrated in application to the hydrogenated amorphous and poly- silicon thin films *[5].* The absolute transmission (T) and reflection (R) measurements were performed with Cary 5E Spectrophotometer using a two-beam scheme with specular reflection attachments which ensure a near normal (~8 °) angle of incidence on the sample.

Table I gives the parameters of the samples used in this study. All samples, except P4, had orientation <100> $\pm$ 0.5°, and were double side polished. Sample P4 had orientation [100] tilted 4 degrees towards [110].

Table I. Parameters for the measured samples.

Notation	Dopant	Resistivity, Ω-cm	Concentration n or p, cm^{-3}	Thickness, μm
N1	Phosph.	0.1-0.3, n	(7-1.5) x 10^{16}	9.8
N2	Phosph.	1.5-2.5, n	(2.5-1.5) x 10^{15}	101
N3	Phosph.	10-30, n	(4.5-1.5) x 10^{14}	199
P1	Boron	<0.015, p	> 5x10^{18}	9.0
P2	Boron	0.2-0.4, p	(9- 6) x 10^{16}	24
P3	Boron	168-464, p	(2.5 - 0.8) x 10^{13}	14.5
P4	Boron	50-200, p	(7 - 2) x 10^{13}	74.9

Because of the high wafer thickness uniformity, typical spectra reveal clearly resolved fringes in optical transmission in the range of small absorption (Figure 1). In reflection, fringes are not resolved to the same degree (Figure 2) because reflection measurements require several times larger area of sample (70-140 mm^2 instead of < 20 mm^2 to measure T). It is obvious, that conventional transmission technique can not be applied in the spectral range where fringes become visible (for this sample at wave lengths greater than 800 nm). Instead, the interference technique has been utilized in this case. The technique has been described previously for a thin film deposited on a substrate [4]. The equations presented in [4] can be easily simplified for our case, since we measure the wafer without substrate. Optical transmission and reflection are given by equations:

$$T= \xi(1-r_1^2)(1-r_2^2)\ e^{-\alpha d}\ ,\ \text{and}\ \ R= \xi\ (r_1^2+2r_1\ r_2\ e^{-\alpha d}\cos 2\delta+ r_2^2\ e^{-2\alpha d}), \qquad (1)$$

where $\xi = (1+ 2r_1\ r_2\ e^{-\alpha d}\cos 2\delta+ r_1^2\ r_2^2\ e^{-2\alpha d})^{-1}$; α and n are the absorption coefficient and the refractive index of material; d is the wafer thickness; $\delta = 2\pi\ n\ d/\lambda$, is the phase thickness of the sample at the wavelength λ, and internal reflection at the top r_1 and bottom r_2 surfaces are given by the Fresnel coefficients of the air-material and material-air interfaces $r_1 = (1- n)/(1 + n)$, $r_2 = (n-1)/(n +1)$. These expressions are valid in the case of a relatively weak absorption coefficient, i.e. when $n^2 >> k^2$, where $k=\lambda\alpha/4\pi$ is the imaginary part of the complex refractive index (the case of so called "absorbing dielectric"). The effect of incomplete fringe resolution can be taken into account by inducing coefficient $b<1$ in the term with $\cos 2\delta$. The value of b can be determine from condition of equity of α in two adjacent transmission extrema and by adjustment of calculated reflection value to the experimental data.

Although we can not use absolute values of reflection for the quantitative analyses, because fringes are not completely resolved, we can use the interference pattern in transmission and reflection for accurately determining the refractive index spectra and the thickness from the relationship

$$n_\lambda\ d = m\ \lambda_m/\ 4, \qquad (2)$$

where n_λ is the refractive index at the wavelength of extrema λ_m. In this procedure we need to know the order of the fringes m, which can be determined from the

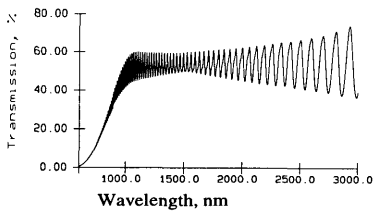

Figure 1. Optical transmission as a function of a wavelength.

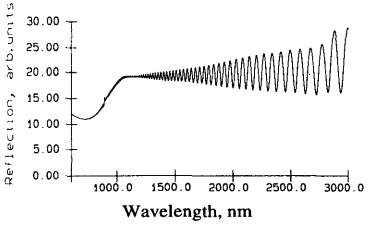

Figure 2. Specular reflection as a function of a wavelength.

wavelengths of two adjacent transmission or reflection extrema in the spectral range where there is no dispersion of n. As it will be demonstrated later, this approximation can be applied between 1.5 and 2.5 μm. Independent measurements of the refractive index from the absolute value of reflection in the range of strong absorption have been used in determining thicknesses of samples, as explained below. We can also use the literature data for n (see, for example [6, 7]) in the same spectral range, where n is practically independent on doping level in non-degenerated material. After the values of the sample thickness and refractive index spectra are found, the absorption coefficient spectra are calculated from the results of transmission experiments. Better results can be obtained at wavelengths of transmission maxima, where most of radiation pass through the sample due to minimum losses for reflection. If fringes are not completely resolved, calculated absorption coefficient in the transmission minima will give artificially negative value, but at the same time, using transmission maxima gives much better results.

In the range of strong absorption, the fringes are not resolved and the average transmission is observed. For this range, the simple expressions usually used in conventional transmission technique for the transmission and the reflection of an optically thick sample are:

$$T= (1-R)^2\ e^{-\alpha d}\ ,\ \ R= [(n-1)/(n+1)]^2. \qquad (3)$$

In this range, the refractive index can be determined directly from the absolute reflection data. These results were used to normalize the dependencies n (λ) calculated from interference pattern using Equation (2), and to determine thicknesses of wafers.

In the intermediate region between multiple reflection and bulk conditions, the interference still influence the results, even if there are no visible fringes. The spectrum of reflection shown in figure 2 has a minimum at λ= 0.8 μm. The position of this minimum depends on the sample thickness, shifting in the direction of higher λ for thicker samples. At wavelengths to the left from this point, the front surface alone contributes to the total reflection since the optical transmission is close to zero. In this range, the drop of R with rising λ is the indicator of the refractive index reducing. This is the spectral range where equations (3) give correct value of refractive index and absorption coefficient. To the right from the minimum, the rising of R indicates that the reflection from the back surface contributes more and more. Using simple equations (3) in this case yield higher then real values of refractive index (see data for the sample N3 in Figure 3 at E< 1.75 eV, (λ>0.7 μm)) and lower then real values of absorption coefficient (Sample P3 in Figure 5 at E< 1.5 eV, (λ > 0.82 μm)). Thus, for this samples, conventional transmission measurements do not give correct values of absorption coefficient near the edge.

EXPERIMENTAL RESULTS

Figures 3, and 4 demonstrate refractive index spectra. Literature data are also included. In the subgap spectral range the dispersion is weak but the refractive index depends on doping level. As it is seen in Figure 4, data for the sample N3 obtained from absolute value of reflection using equation (3) give fictitious rising of refractive index at energies less than 1.8 eV where absorption becoming week and the bottom surface of the sample influences results.

Figures 5 and 6 demonstrate dependence of absorption coefficient on energy for n- and p-type Si membranes in the extended energy range. Data for the sample N3 calculated from equation (3) demonstrate fictitious drop of absorption at E< 1.5 eV (λ > 0.8 μm) indicating necessity of using interference equation (1). Formulae (7) and (8), both start giving wrong results in this range even although transmission is still very low (at the level of 10-15 %) and fringes are not resolved. The wavelength at which this occurs depends on the sample thickness. For more thick samples this critical λ shifts in the direction of small absorption coefficient and large wavelength.

At λ > 1.1 μm, which correspond to the subgap energy range (photon energy E < E_g), the absorption is related to impurities and defects. There is a trend of rising this background absorption with reducing the sample thickness. All thin samples with thicknesses below 25 μm which are polished by additional chemical methods have much higher subgap absorption. This high level background absorption, in some cases independent of photon energy, might indicate the presence of surface defects in these samples. More measurements, including undoped samples, have to be done to receive quantitative results on subgap absorption due to surface and bulk electronic defects

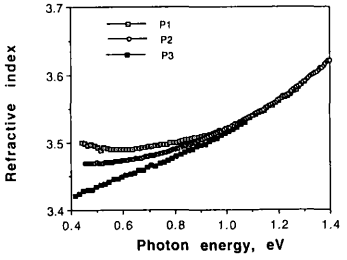

Figure 3. Refractive index spectra of P-Si samples with different doping level near the edge.

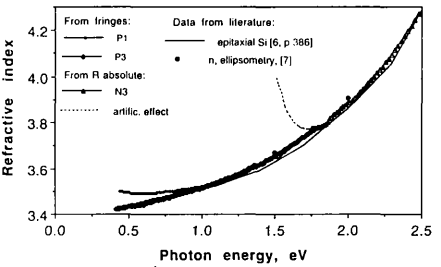

Figure 4. Refractive index spectra of P- and N-Si in the extended energy range.

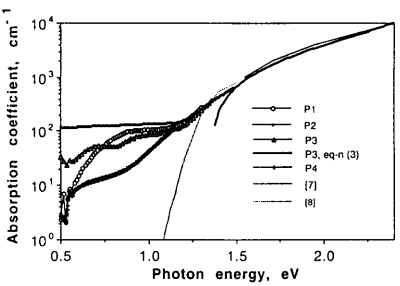

Figure 5. Absorption coefficient spectra of P-Si samples.

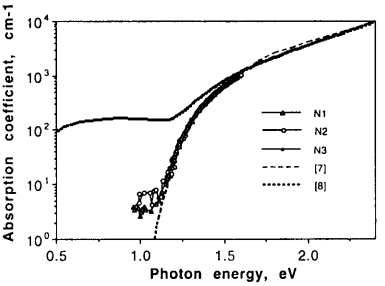

Figure 6. Absorption coefficient spectra of N-Si samples.

and impurities.

For the purposes of the analysis of absorption near the edge, we can use a first estimate of this wide range background absorption as a constant and extract it from the total spectrum. The results of this simple procedure for the sample N2 in Figure 7 demonstrate a good agreement with earlier data on monocrystalline Si [8]. The quantitative analysis of the rectified spectra is still complicated due to contribution of impurities and phonons. We, however, can approximate the first indirect gap absorption by expression

$$\alpha = B(E- E_0)^2 / E \qquad (4)$$

and extract parameters from the plot of $(\alpha E)^{1/2}$ versus E as shown in Figure 8. In the low-energy region 1.15 -1.5 eV, the data are close to linear dependence which permit to receive an optical gap E_0 and a constant B listed in the Table 2. Since transitions with phonon emission contributes most of all in this absorption, we expect that E_0 is lightly higher than the first fundamental gap in Si.

There is the change in the slope of $(\alpha E)^{1/2}$ at energy around 1.5 eV. This, not very well distinct change, has been earlier observed in [9, 10] and has been attributed to the second indirect $\Gamma_{25'}$ --> L_1 transition to the upper conduction band minima. The threshold of this transition has been determined by subtracting of the extrapolated linear value of the first indirect transition from the experimental data and plotting the difference versus E. We applied the same procedure for the analysis of our data. The resulting difference is shown in Figure 7. The similarity between this second edge and the first one is observed. The energy difference between these two edges is about 0.4 eV which can be found simply by the shift of the second edge curve. Parameters of the second edge E_{02} and a constant B_2 have been determined using the same equation (4) (see Table II). It is better to use for this procedure N-type samples, since transitions from impurities closed to the valence band mask the threshold and the interpretation of results is not so clear. Thus we could use only data from one N-type sample and the accuracy of parameters is not very good since the change in the slope is not large. Nevertheless, in complete accordance with the interpretation of [9], it is clear that these transitions are indirect. For the reason which will be discussed later, and because of the similarity of the first and the second indirect transitions, we assign this second one to the transition from $\Gamma_{25'}$ into conduction band minima situated approximately at X points of the Brillouin zone along the X - K direction. The change in absorption coefficient at E_{02} is not large and is very smooth. The threshold energy of this transition seems to be less than 1. 63 eV. This can explain why the second transition has not been detected in [2].

Table II. Parameters for optical transitions.

Sample	E_0, eV	B, $cm^{-1} eV^{-1}$	E_{02}, eV	B_2,$cm^{-1} ev^{-1}$	E_{03}, eV	B_3, $cm^{-1} ev^{-1}$
N2	1.145	7750				
N3	1.15	7650	1.50-1.65	4500-7000	1.9-2.00	30000-35000

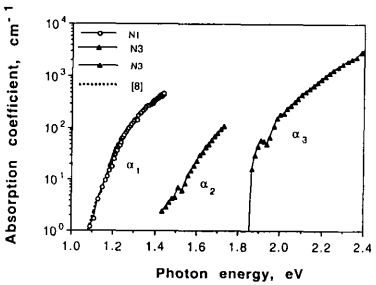

Figure 7. Three components of the interband absorption near the edge.

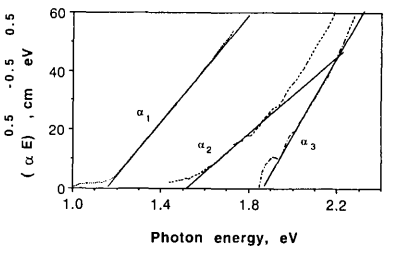

Figure 8. Tauc plots for three components of optical absorption .

At higher energies, the much more pronounced break in the slope of $(\alpha_2 E)^{1/2}$ near the energy E_{03} has been found. Since we measure absorption of one sample in a very extended energy range, we are enable to repeat the above procedure, to extract absorption due to the second transitions, and to receive parameters of the third transitions. This is again indirect band transition with the threshold $E_{03}=1.95 \pm 0.1$ eV, and with the oscillator strength of about 5 times larger than that of the first transition ($B_3 = 3x10^4$ $cm^{-1}eV^{-1}$). The threshold energy for this transition is very close to the theoretical threshold at the $\Gamma_{25'}$ --> L_1 critical point (see review in [9]) .

We have measured only one thin N-type sample. Thus again, much more measurements have to be done using undoped material with low level of compensation to receive more accurate information regarding to the upper bands in Si.

CONCLUSIONS

The excellent quality ultrathin silicon membranes have been used to study the optical properties of Si in a wide energy range. The interference technique gives good agreement with results obtained by conventional transmission and reflection measurements in the range of high absorption, and permits precise optical characterization in the subgap range, where conventional methods do not work well. The optical properties of ultrathin silicon membranes at the edge correlate well with optical properties of conventional crystalline silicon material.

The absorption spectrum analysis from measurements of the same sample in an extended energy range give new information regarding transitions into upper conduction bands.

REFERENCES

1. K.S. Sieh, P.V.Smith, Phys. Status Solidi (b), 129, p.259 (1985).
2. J. Geist, A. Migdall, and H. Baltes, Applied Optics, V29, N24, 3548-3554 (1990).
3. J.Geist, A.R. Schaefer, J.F. Song, Y. H. Wang, and F. Zalewski, J. of Research of the National Institute of Standards and Technology, V95, N5, 549 (1990).
4. T. Globus, G. Gildenblat, S. Fonash, MRS Proc., 406, p.313 (1996).
5. T. Globus, International Semiconductor Device Research Symposium, Proc. Vol.1, 27, Charlottesville, VA, Dec. 1995.
6.Physics of group IVelements & III-Vcompounds ed by O.Madelung, p.386, Fig.117, ch 1.2-Silicon (1981).
7. Landolt-Bornstein, Numerical Data and Functional Relationships in Science and Technology. Band17, p.20 (1985).
8. G. D. Cody, MRS Symp. Proc. V.192, p. 113 (1990).
9. R. A. Forman, W. R Thurber, and D. E. Aspnes, Solid State Comm. V. 14, pp. 1007 (1974).
10. H. A. Weakliem, D. Redfield, J. Applied Phys., 50 (3), 1491 (1979).